# FORMATION OF REACTIVE OXYGEN SPECIES (ROS) AND THEIR EFFECT ON DNA

S. Reuter[1,4], K. Wende[1,4], J. Winter[1,4], S. Blackert[2],
M. Harms[2], K Masur[1,4],V. Schulz-von der Gathen[3], T. v.Woedtke[4], K.D. Weltmann[4]

[1]*Centre for Innovation Competence plasmatis, 17489 Greifswald*
[2]*Ernst-Moritz-Arndt University Greifswald Institute for Pharmacy, 17489 Greifswald*
[3]*Ruhr-University Bochum, Institute for Experimental Physics II, D-44780 Bochum,*
[4]*Leibniz Institute for Plasma Science and Technology e.V. (INP),17489 Greifswald*

***Abstract:*** The interdisciplinary field of plasma medicine requires a thorough investigation of the reaction pathways from the plasma sources down to the cellular level. The work presents state of the art optical diagnostics such as two-photon absorption laser induced fluorescence spectroscopy of reactive oxygen species (ROS) and their reaction kinetics in an atmospheric pressure plasma source. Parallel to these investigations on fundamental processes in the plasma chemistry, the effect of reactive oxygen species on cellular DNA of plasma treated HaCaT cells is investigated. The ROS accumulation within the cells is determined by oxidation of $H_2$DCFDA. Subsequently the ROS effect on the integrity of the cellular DNA is measured by single cell electrophoresis.

***Keywords:*** APP, Reactive Oxygen Species, Optical Plasma Diagnostics, HaCaT Cells

## 1. Introduction

The recent progress in the development and research of non equilibrium atmospheric pressure plasmas (APPs) with high reactive species densities at low gas temperature has made plasma-treatment of living tissue possible and promises an efficient and improved treatment of infected or chronic wounds as well as hard to heal skin diseases [1]. In plasma - cell/tissue interaction secondary effects play a crucial role. Most mammalian cells require a liquid surrounding in order to survive – therefore it is always via an interface, namely the extracellular physiological environment, that the plasma influences the cell. For a thorough analysis of this plasma - cell environment interaction a detailed quantitative analysis of the discharges reactive components is required. This work presents methods of optical plasma diagnostics suited for investigating the reactive oxygen species (ROS) in atmospheric pressure plasmas together with methods to investigate APPs effect on cellular DNA. Plasma diagnostics are performed exemplarily on a so-called APPJ, biologic experiments are performed using both a kINPen and a surface dielectric barrier discharge (DBD). All three plasma sources are briefly described in the following.

## 2. Plasma Sources

The kINPen is a concentric plasma jet. In the center of a quartz capillary (inner diameter 1.6 mm) a pin-type electrode (1 mm diameter) is mounted. In the continuous working mode, a high-frequency (HF) voltage (1.1 MHz, 2-6 kVpp) is coupled to the pin-type electrode [2]. The carrier gas in this case is argon with small molecular admixtures. The atmospheric pressure plasma jet (APPJ) is a capacitively coupled radio frequency excited plasma source, which can be operated at ambient conditions. The planar setup consists of two water cooled planar stainless steel electrodes (length 80 mm, width 40 mm), one of which is grounded, while the other is driven by a 13.56 MHz RF-power source. The electrode gap is 1.1 mm. A more detailed description of the APPJ can be found in [3]. The surface dielectric barrier discharge (DBD) consists of a back plate electrode, a dielectric and a structured surface electrode covered in alumina [4]. It is operated with a frequency of 2 kHz and a voltage of 10 kHz in open air.

## 3. Plasma Diagnostics and Results

The atomic oxygen density distribution in the effluent of the plasma jet is determined by two-photon absorption laser induced fluorescence (TALIF)

spectroscopy. Tunable UV-laser radiation is used to excite oxygen atoms by simultaneous absorption of two UV-photons. The fluorescence radiation emitted when the atoms revert to an energetically lower state is measured in order to gain information about the atomic oxygen density. A detailed setup and measurement description is presented in [2]. For the measurements, the APPJ is placed in a recipient filled with one atmosphere of helium. A frequency doubled Nd:YAG-laser pulsed at 10 Hz is used to pump a dye laser, equipped with a frequency tripling unit, in order to obtain the tunable UV radiation at about 225 nm for two-photon excitation of ground state oxygen atoms. The fluorescence of the oxygen atoms (~845 nm) is detected perpendicular to the exciting laser beam with a photomultiplier.

The ozone density in the APPJ's effluent is determined by UV-absorption spectroscopy. The λ=253.7 mercury line of a Hg/Ar lamp is used for the UV-absorption measurements. The UV spectrum is recorded with a 0.2 m monochromator. The density is calculated by Beer's law taking into account the absorption cross section of ozone λ @ 253,7nm = 1.14 x $10^{17}$ $cm^2$[5]. The measurements in this study are line of sight measurements along the long (x-)axis of the jet.

A relative density distribution of singlet metastable molecular oxygen $O_2(b^1\Sigma_g^+)$ in the APPJ's effluent is derived from optical emission spectroscopy (OES). The spectroscopic setup is described in detail in [2]. The emission band of $O_2(b^1\Sigma_g^+)$ at 762 nm is shown in fig. 1 (transition $(b^1\Sigma_g^+)$ ν=0 → $(X^3{}_g^-)$ ν=0)

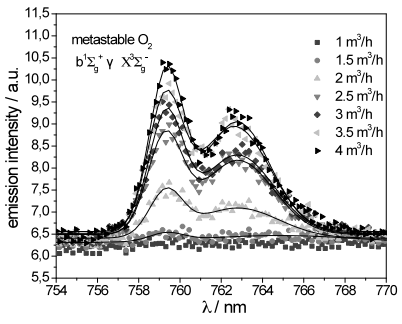


Fig. 1: OES on $O_2(b^1\Sigma_g^+)$ at 4 mm distance from the jet's nozzle in helium atmosphere at 150Watt RF-power and 0.5 vol% O2-admixture for different total gas fluxes

For a chemical model of the processes in the plasma jet's effluent apart from helium, five oxygen species (O, $O_2$, $O_3$, $O_2(a^1\Delta_g)$, $O_2(b^1\Sigma_g^+)$) are relevant. As starting parameters for the model, their respective initial densities are taken from the measurements. UV-absorption measurements on ozone as well as optical emission spectroscopy on $O_2(b^1\Sigma_g^+)$, and TALIF-measurements of the atomic oxygen density yield the input parameters for these reactive oxygen species. The density of metastable $O_2(a^1\Delta_g)$ is in the same magnitude as the atomic oxygen density [6] and the initial density of molecular oxygen can be derived from the experimental conditions.

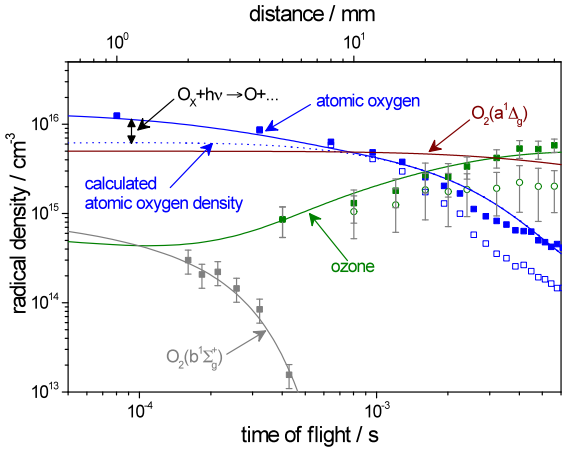


Fig. 2: Comparison of chemical model calculations with the measured oxygen species' densities. Solid symbols represent the on-axis reactive species' densities with diffusion effects considered. Open symbols for atomic oxygen and ozone represent the measured on-axis densities

The final results from the model calculations compared with the measured oxygen species' densities (O, $O_3$, and $O_2(b^1\Sigma_g^+)$) are depicted in fig 2. Open symbols represent the measurements and solid symbols are the densities with diffusion effects taken into account. The relative $O_2(b^1\Sigma_g^+)$-density as derived from the OES-measurements is reconciled with the density distribution from the model calculations to achieve an absolute $O_2(b^1\Sigma_g^+)$-density. The progression of measured and calculated oxygen species' densities is in excellent agreement. The processes in the effluent can be summarized as follows: Ozone is produced by the three body reaction of atomic and molecular oxygen with a third reaction partner. A high consumption of ozone close

to the nozzle is mainly due to reaction with $O_2(b^1\Sigma_g^+)$. The rapid decrease of the $O_2(b^1\Sigma_g^+)$-density due to this reaction explains the observed increase of the ozone density towards higher distances from the nozzle. The high density of molecular oxygen in the order of $10^{17}$ $cm^{-3}$ remains practically constant. The model calculations also show that the $O_2(a^1\Delta_g)$-density decreases slowly (due to the metastables' high lifetime) and is still considerably high at several centimeters distance from the nozzle. The likewise slow decrease of the atomic oxygen density can partially be explained by reaction of ozone with $O_2(a^1\Delta_g)$, producing atomic oxygen. However, the comparison shows that the initial atomic oxygen density for the model has to be assumed lower than the measured density, in order to achieve agreement towards higher time of flight. The deviation between calculated and measured atomic oxygen density close to the nozzle can be seen in fig. 2. In our preceding study [2], (V)UV-radiation was identified as a means of an energy transfer from the APPJ's discharge region, possibly generating surplus atomic oxygen in the effluent. (V)UV radiation – and accordingly its effect on the atomic oxygen density – is strongest close to the nozzle. The difference between measured radical densities and results from the model calculations close to the nozzle is resolved, when atomic oxygen produced by (V)UV-photo dissociation is added to the calculated O-density.

## 4. Cellular Diagnostics and Results

To gain insight into intracellular effects of atmospheric pressure plasma treatment, DNA damage detection was carried out using single cell electrophoresis (Comet assay) and ROS detection by oxidation of $H_2$DCFDA. Cells were loaded with the membrane permeable leukodye $H_2$DCFDA (10µM) within 30 min after dielectric barrier discharge treatment in air. After its oxidation by ROS, fluorescence was measured (excitation 485nm/emission 520nm) [7] (fig. 3). Apart from treatment time dependency (120s > 100s etc.) a significant influence of the type of cell culture medium was observed. When using Iscove's modified Dulbecco's Medium (IMDM) instead of Roswell Park Memorial Institute 1640 (RPMI) for the same experiment, intracellular oxygen radical densities dropped markedly. Oxygen radical absorbance capacity assay (ORAC) revealed a much higher effectivity (4.7fold) of IMDM compared to RPMI (data not shown). For higher sensitivity subsequent experiments were carried out using RPMI.

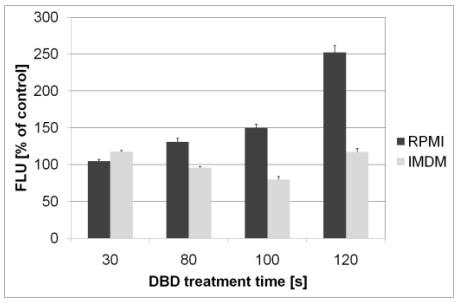


Fig. 3: Intracellular ROS detection ($H_2$DCFDA, 485/520) 30 min after HaCaT DBD treatment in air.

Various effects of reactive oxygen species need to be considered: Apart from their role as second messenger (NO, $O_2^{\cdot -}$) [8] an interaction with cellular macromolecules such as DNA is possible. In order to detect DNA deterioration, treated cells were placed in agarose gel, lysed, and the remaining DNA was forced to migrate in an electric field (single cell electrophoresis). The DNA migration velocity depends on number and frequency of DNA lesions. The comets formed during migration are a measure for DNA deterioration and can be quantified by the tail moment. [9] Treatment of HaCaT cells with the kINPen operated with argon at ambient conditions showed a treatment time dependant increase of the tail moment, indicating DNA single strand breaks or DNA oxidation (fig. 4).

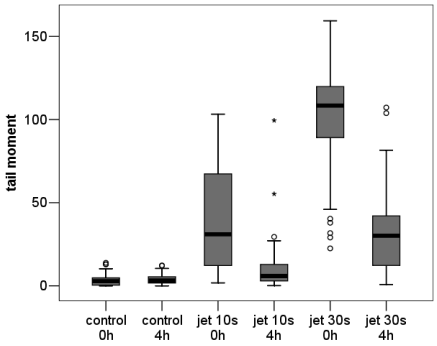


Fig. 4: Alkaline Comet assay. kINPen treatment with argon in air, HaCaT cells adherent. Tail moment indicates DNA damage.

However, tail moments decrease after prolonged incubation time, indicating DNA damage repair,

and/or depletion of damaged cells. This observation needs to be verified in future work.

When treating HaCaT cells in suspension with the dielectric barrier discharge in air, tail moments were generally lower than after kINPen treatment. This indicates a reduced number of DNA lesions and hence less ROS within the HaCaT cells after treatment with this plasma source (fig. 5).

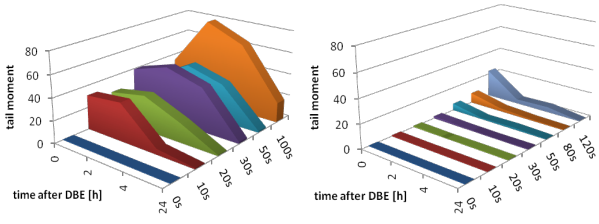


Fig. 5: Alkaline Comet assay. DBD treatment in air, cells suspendend in either RPMI (left) or IMDM (right). Tail moment indicates DNA damage.

Cells treated suspended in RPMI, however, displayed the expected response (treatment time dependent increase of tail moment, tail moments inversely depend on incubation time). Exchanging RPMI for IMDM, tail moments (and thus DNA single strand breaks) dropped almost to control level, even at the highest treatment times. This observation confirms the assumption of a higher radical scavenging activity of IMDM and its implication for in vivo situations (see below).
When using the neutral variant of the Comet assay [10], only few DNA double strand breaks were detected for high treatment times (kINPen, 80s). The same apparent recovery during further incubation as in the case of single strand breaks was observed.

The biological effects observed depended on the type of plasma source, treatment time and type of nutrient medium. With increasing time after treatment, DNA deterioration decreases. It needs to be verified in future – e.g. by normalization of the results to total cell count – whether the results show a selective cell death or repair of DNA. As the type of nutrient medium plays a major role, treatment in vivo may lead to different results regarding DNA damage because the nutrient supply in vivo differs from vitro culture. Additionally, regular healthy skin consists of several layers. Especially the outer layer (stratum corneum) consisting of dead cells will not be affected by DNA damaging agents. Regarding applications, the influence of plasma is of interest only for cells beneath this layer (at a depth of around 150 µm). The experiments described will help to define a threshold treatment time for future skin treatment.

*Acknowledgements:* The Centre for Innovation Competence *plasmatis* would like to thank the BMBF for funding. Part of this work was supported within the research project "plasma enhanced surface modification of biomedical relevance" by the MSWF of NRW and within the joint research project "Campus PlasmaMed" by the German Federal Ministry of Education and Research.

## References

[1] G. Daeschlein, S. Scholz, A. Arnold, T. von Woedtke, E. Kindel, M. Niggemeier, K.-D. Weltmann, and M. Jünger, Plasma Science, 2010, 38, 2969

[2] K.-D. Weltmann, E. Kindel, T. von Woedtke, M. Hähnel, M. Stieber, and R. Brandenburg, Pure Appl. Chem., 2010, *82*, 1223

[3] S. Reuter, K. Niemi, V. Schulz-von der Gathen, and H. F. Döbele Plasma Sources Sci. Technol., 2009, 18, 015006

[4] M. Hähnel, T. von Woedtke, K.-D. Weltmann, Plasma Proc. Pol., 2010, 7, 244

[5] C. Parisse, J. Brion, and J. Malicet. Chem. Phys. Lett., 1996, 248, 31

[6] J. Y. Jeong, J. Park, I. Henins, S. E. Babayan, V. J. Tu, G. S. Selwyn, G. Ding, and R. F. Hicks. J. Phys. Chem. A, 2000, 104, 8027

[7] E. Eruslanov, S. Kusmartsev in D. Armstrong (ed.), Advanced Protocols in Oxidative Stress II, Methods in Molecular Biology, vol. 594 DOI 10.1007/978-1-60761-411-1_4

[8] T. Finkel: Current Opinion in Cell Biology 1998,10, 248

[9] N.P. Singh, M.T. McCoy, R.R. Tice, E.L. Schneider Exp. Cell Res. 1988, 175, 184

[10] P.L. Olive, P. Banath, Int. J. Radiat. Biol. 1993, 64, 349